Since January 2020 Elsevier has created a COVID-19 resource centre with free information in English and Mandarin on the novel coronavirus COVID-19. The COVID-19 resource centre is hosted on Elsevier Connect, the company's public news and information website.

Biosensors and Bioelectronics 203 (2022) 114032

Contents lists available at ScienceDirect

Biosensors and Bioelectronics

journal homepage: www.elsevier.com/locate/bios

An encodable multiplex microsphere-phase amplification sensing platform detects SARS-CoV-2 mutations

Zecheng Zhong [a,1], Jin Wang [a,b,1], Shuizhen He [c,1], Xiaosong Su [d], Weida Huang [a], Mengyuan Chen [a], Zhihao Zhuo [a], Xiaomei Zhu [a], Mujin Fang [a], Tingdong Li [a], Shiyin Zhang [a,*], Shengxiang Ge [a,**], Jun Zhang [a], Ningshao Xia [a,b,e,***]

[a] State Key Laboratory of Molecular Vaccinology and Molecular Diagnostics, National Institute of Diagnostics and Vaccine Development in Infectious Diseases, School of Public Health, Xiamen University, Xiamen, 361102, China
[b] School of Life Sciences, Xiamen University, Xiamen, 361102, China
[c] Xiamen Haicang Hospital, Haiyu Road, Xiamen, 361026, China
[d] Xiang'an Hospital of Xiamen University, Xiang'an East Road, Xiamen, 361102, China
[e] The Research Unit of Frontier Technology of Structural Vaccinology of Chinese Academy of Medical Sciences, Xiamen, 361102, China

ARTICLE INFO

Keywords:
SARS-CoV-2
Mutation
Encodable
Multiplex amplification
Variant

ABSTRACT

SARS-CoV-2 variants of concern (VOCs) contain several single-nucleotide variants (SNVs) at key sites in the receptor-binding region (RBD) that enhance infectivity and transmission, as well as cause immune escape, resulting in an aggravation of the coronavirus disease 2019 (COVID-19) pandemic. Emerging VOCs have sparked the need for a diagnostic method capable of simultaneously monitoring these SNVs. To date, no highly sensitive, efficient clinical tool exists to monitor SNVs simultaneously. Here, an encodable multiplex microsphere-phase amplification (MMPA) sensing platform that combines primer-coded microsphere technology with dual fluorescence decoding strategy to detect SARS-CoV-2 RNA and simultaneously identify 10 key SNVs in the RBD. MMPA limits the amplification refractory mutation system PCR (ARMS-PCR) reaction for specific target sequence to the surface of a microsphere with specific fluorescence coding. This effectively solves the problem of non-specific amplification among primers and probes in multiplex PCR. For signal detection, specific fluorescence codes inside microspheres are used to determine the corresponding relationship between the microspheres and the SNV sites, while the report probes hybridized with PCR products are used to detect the microsphere amplification intensity. The MMPA platform offers a lower SARS-CoV-2 RNA detection limit of 28 copies/reaction, the ability to detect a respiratory pathogen panel without cross-reactivity, and a SNV analysis accuracy level comparable to that of sequencing. Moreover, this super-multiple parallel SNVs detection method enables a timely updating of the panel of detected SNVs that accompanies changing VOCs, and presents a clinical availability that traditional sequencing methods do not.

1. Introduction

Coronavirus disease 2019 (COVID-19) caused by severe acute respiratory syndrome coronavirus 2 (SARS-CoV-2) has had a devastating impact globally on public health and the economy (Dorn et al., 2020). The emergence of new SARS-CoV-2 genetic variants has further exacerbated the COVID-19 pandemic (Grubaugh et al., 2021). Based on the risk posed to global public health, the World Health Organization (WHO) classified SARS-CoV-2 variants as variants of interest (VOIs) and variants of concern (VOCs) (World Health Organization, 2021). VOIs refer to variants that show a rising prevalence in many regions of the world and may cause a pandemic. Based on their compliance with VOIs,

* Corresponding author.
** Corresponding author.
*** Corresponding author. State Key Laboratory of Molecular Vaccinology and Molecular Diagnostics, National Institute of Diagnostics and Vaccine Development in Infectious Diseases, School of Public Health, Xiamen University, Xiamen, 361102, China.
E-mail addresses: zhangshiyin@xmu.edu.cn (S. Zhang), sxge@xmu.edu.cn (S. Ge), nsxia@xmu.edu.cn (N. Xia).
[1] These authors contribute equally to this paper.

https://doi.org/10.1016/j.bios.2022.114032
Received 3 December 2021; Received in revised form 17 January 2022; Accepted 20 January 2022
Available online 31 January 2022

VOCs are variants with increased transmission and virulence that will affect the current diagnosis, vaccine, and treatment effects, as well as seriously threaten public health safety. Therefore, it is critically important to monitor and track VOCs globally to control the spread of COVID-19 (World Health Organization, 2021).

At present, several methods of detecting SARS-CoV-2 have been developed. Some of these methods based on viral gene detection (Zhang et al., 2020) or viral protein detection (Ahmadivand et al., 2021). Novel sensors based on the above two methods have been developed as well (Kaushik, 2021; Mujawar et al., 2020; Sharma et al., 2021). These methods further enhance SARS-CoV-2 testing sensitivity, specificity or on-site detection availability. Viral gene detection via real-time fluorescent quantitative polymerase chain reaction (qPCR) is the gold standard for the detection of SARS-CoV-2 (Ai et al., 2020; Corman et al., 2020). Although qPCR is currently widely used for mass screening and testing, it fails to distinguish between the wild-type SARS-CoV-2 and its new variants (Afzal, 2020). Moreover, emerging variants will subsequently affect the sensitivity of qPCR (Osorio and Correia-Neves, 2021; Tahamtan and Ardebili, 2020; Wang et al., 2020). Whole-genome sequencing (WGS) is an accurate method to detect, monitor, and track VOCs (Vandenberg et al., 2021). However, the extensive application of WGS in large-scale testing programs and resource-poor areas is limited due to high associated costs, long sample processing time, and low sample throughput (Esbin et al., 2020; Jayamohan et al., 2021). Therefore, qPCR and WGS are unsuitable for the large-scale monitoring and tracking of VOCs. Detection methods suitable for large-scale testing must be developed to enable public health systems to monitor and manage VOCs (Kumar et al., 2021).

VOCs contain multiple single-nucleotide variants (SNVs) at key points of the receptor-binding region (RBD) that enhance infectivity and transmission, as well as cause immune escape (Harvey et al., 2021). Therefore, a multiplex detection method is required to detect such SNVs. Currently, amplification refractory mutation system PCR (ARMS-PCR) is most widely used to detect SNVs (Little, 2001; Mishra et al., 2017). It uses the 3′-end of primers to block amplification, thus requiring a set of dedicated primers and probes for each SNV. The use of numerous sets of primers and probes in a single multiplex reaction may significantly increase the probability of non-specific amplification, thereby leading to a decrease in sensitivity and specificity (Elnifro et al., 2000). Furthermore, when new SNVs appear, the new detection targets need to be added to the system, and a considerable amount of rescreening work needs to be carried out to update primer and probe sets. The number of SNVs detected in one reaction tube will also be limited by the number of fluorescent channels of the qPCR instrument; usually, instruments only feature five to six fluorescent detection channels (Khodakov et al., 2021). A parallel multi-tube detection model was developed for the multiplex detection of SNVs to avoid these issues (Board et al., 2008). However, this method could only detect one to two SNV loci in each reaction tube, resulting in a labor-intensive, expensive, and inefficient detection system. Therefore, ARMS-PCR is limited in detecting multiple SNVs of VOCs in large-scale tests, creating an urgent need for an efficient multiplex detection assay to identify SNVs in VOCs.

Here, we developed a multiplex microsphere phase amplification (MMPA) sensing platform for the detection of SNVs. This platform executed super multiple non-interference parallel amplification using microspheres encoded by AMRS primers and achieved multiple detection through a strategy involving the fluorescence encoding of microspheres and reporting probes. By coating the microsphere surface with SNV-specific ARMS primers, MMPA limited the ARMS-PCR to a defined area on the microsphere. Moreover, the amplifications separated in space, avoiding mutual interferences between amplified primers. Therefore, MMPA could effectively amplify different target sequences around primers coated on a distinct microsphere surface, consequently achieving the super-multiplexed parallel amplification of DNA targets, which would solve the problem of mutual interference between different target primers in multiple amplification. Furthermore, we combined the fluorescence of microspheres with that of reporting probes to encode the amplified signals of different targets and eliminate insufficient multiple detection channels as a limitation. Once the reactions involving the microspheres were completed, the fluorescence signals of microspheres and the reporting probes were analyzed via a dual fluorescence decoding strategy to identify different SNVs. Using the fluorescent dye coded strategy, up to 500 fluorescence-coded microspheres can be prepared, with primers for different targets labeled on specific microspheres. As each labeled microsphere can be used to detect one target, hundreds of targets can be simultaneously detected in theory, thus effectively solving the problem of insufficient detection channels in multiplex detection systems. In this study, the programmable, high-throughput, multiplex detection method to identify 10 key SNVs in the RBD of VOCs can be used to monitor and track SARS-CoV-2 variants.

2. Materials and methods

2.1. Wild-type and mutant SARS-CoV-2 RNA

The natural wild-type SARS-CoV-2 and Delta variant RNA used in this study were pre-extracted and kindly donated by Shantou University. Plasmids containing the RBD gene of mutant SARS-CoV-2 along with a T7 promoter sequence were synthesized by Sangon (Shanghai, China). Single-stranded RNA was generated from the T7 promoter using T7 RNA polymerase (NEB, USA). Next, plasmid DNA was removed from RNA samples using RNase-free DNase I (Takara, Dalian, China), and the RNA was utilized in subsequent analyses.

2.2. Nucleic acid extraction

Human coronavirus 229E (2.37×10^7 $TCID_{50}$/mL), human coronavirus OC43 (5.72×10^7 $TCID_{50}$/mL), human coronavirus NL63 (8.24×10^7 $TCID_{50}$/mL), human coronavirus HKU1 (3.32×10^7 $TCID_{50}$/mL), influenza A (H3N2, 1.56×10^7 $TCID_{50}$/mL), influenza B (Victoria Lineage, 4.68×10^7 $TCID_{50}$/mL), and respiratory syncytial virus (RSV) A2 (1.43×10^7 $TCID_{50}$/mL) were pre-inactivated. RNA was extracted from 200 μL of viral cultures, and nasal swab eluent spiked with pseudovirus using a magnetic bead nucleic acid extraction kit (GenMagBio, Beijing, China) according to the manufacturer's instructions. RNA was eluted with 50 μL of DEPC-treated water, and the concentration and quality were measured using the Multiskan Spectrum spectrophotometer (Thermo Scientific, USA).

2.3. Primer and probe design

We downloaded the RBD sequence of wild-type and different SARS-CoV-2 variants from GISAID (https://www.gisaid.org/). Sequences were aligned using ClustalW. A pair of universal outer flanking primers was designed, and the produced resulting amplicon contained all the 10 SNVs explored in this study. The 3′ end nucleotide of the inner forward primers were designed to correspond to the variation sites, and the 5′ end was modified with amine-C36. The probes were modified with 6-carboxytetramethylrhodamine (TAMRA) at both the 5′ end and 3′ ends to enhance the signal-to-noise ratio. All primers and probes sequences (Table S1, Supplementary Material) were purchased from Sangon, China.

2.4. The conjugation of primers to microspheres

Primers modified with amine-C0, C12, C24, or C36 at the 5′ end were covalently linked to carboxylated MicroPlex® microspheres (Luminex, USA) according to the manufacturer's instructions. To detect the 10 RBD SNVs, we chose 20 fluorescence-coded microspheres that were distinguished by two distinct luciferin ratios, each of the microspheres emits a unique wavelength of excitation light when illuminated by a red laser; 20 forward primers, including primers specific to wild-type and mutant

SARS-CoV-2, were separately coupled to 20 different microspheres.

2.5. Detection of multiple SARS-CoV-2 SNVs

Liquid phase PCR was performed using a pair of universal outer flanking primers to pre-enrich the target sequence. Each 25 μL reaction tube contained 1 × PCR buffer (Takara, Dalian, China), 200 μM dNTPs, 2 U TaKaRa Taq™ Hot Start DNA polymerase (HS Taq) (Takara, Dalian, China), 4 U TransScript Reverse Transcriptase (TransGen Biotech, Beijing, China), 0.04 μM of forward primer, 0.4 μM of reverse primer, and 5 μL of template. Thermal cycling involved a reverse transcription step at 50 °C for 10 min, an enzyme activation step at 95 °C for 5 min, followed by 40 cycles at 95 °C for 15 s and 55 °C for 45 s. PCR was performed using a T100 thermal cycler (Bio-Rad, USA).

MMPA was performed in a volume of 25 μL containing 1 × PCR buffer (Takara, Dalian, China), 200 μM dNTPs, 10 U HS Taq (Takara, Dalian, China), 1 U SpeedSTAR™ HS DNA polymerase (SS Taq) (Takara, Dalian, China), 20 fluorescence-coded microspheres (each coupled with a specific forward primer; approximately 4.688 × 10^2 microspheres for each primer), 0.4 μM of a universal reverse primer, and 5 μL of pre-enriched single-stranded DNA. PCR was carried out as follows: reactions were denatured at 95 °C for 5 min followed by 60 cycles of 95 °C for 20 s, 55 °C for 30 s, and 72 °C for 30 s, and finally followed by a 5 min extension step at 72 °C.

Universal double-ended TAMRA-modified probe (0.04 μM) was added to the products. Hybridization procedures consisted of an initial step at 95 °C for 5 min, followed by 55 °C for 5 min. Next, 125 μL of 1 × PCR buffer (Takara, Dalian, China) was added, and the microspheres were analyzed for their internal color and external TAMRA reporter fluorescence using a Luminex 200 (Luminex Corp., TX, USA). The median reporter fluorescence intensity (MFI) of each microsphere was computed, and the cutoff value for a positive result was set as twice the MFI value of the negative control. We recast the formulas presented in the reference (Chuenkova and PereiraPerrin, 2009; Ju et al., 2015); the standardized formula used for the relative difference in fluorescence between the wild-type and mutants was as follows: $\log_2 |(\mathrm{MFI}_{\mathrm{mutant}} - \mathrm{MFI}_{\mathrm{background}})/(\mathrm{MFI}_{\mathrm{wild}} - \mathrm{MFI}_{\mathrm{background}})|$.

2.6. Reverse transcription quantitative PCR

Reverse transcription quantitative PCR (RT-qPCR) was carried out using a master mix reagent consisting of 50 mM Tris-HCl (pH 8.5), 2 mM $MgSO_4$, 70 mM CH_3COOK, 200 μM dNTPs, 2 U TaKaRa Taq™ HS DNA polymerase (Takara, Dalian, China), 8 U TransScript Reverse Transcriptase (TransGen Biotech, Beijing, China), 0.4 μM of each primer, and a TaqMan probe for SARS-CoV-2 (Table S1). The thermal cycling program included a reverse transcription step at 50 °C for 10 min, an enzyme activation step at 95 °C for 5 min, followed by 40 cycles at 95 °C for 15 s and 55 °C for 45 s. PCR reactions were performed on a CFX96TM system (Bio-Rad, USA). For EvaGreen® RT-qPCR, all parameters were identical to TaqMan RT-qPCR except for substituting 0.4 μM probe for 0.8 × EvaGreen® dye (Biotium, USA).

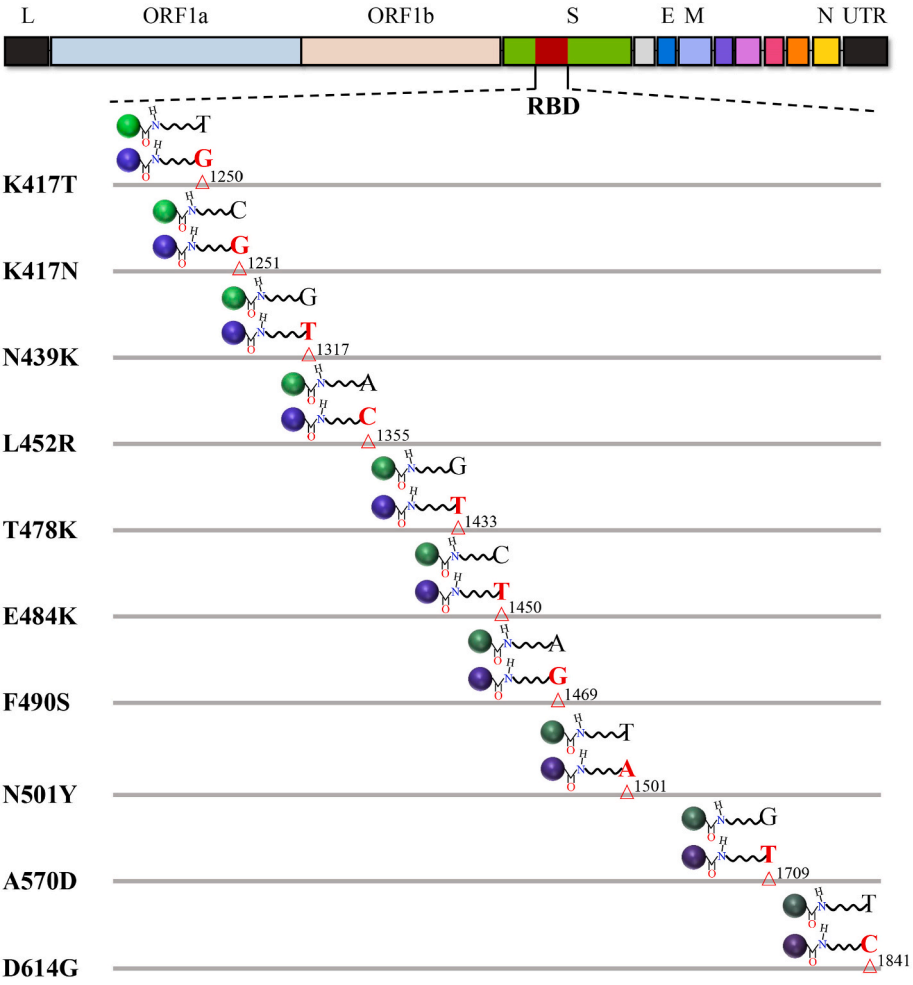

Fig. 1. Ten SNVs of SARS-CoV-2 variants. For each SNV, one wild-type and one mutant forward primer were designed and coated on separate microspheres. SNV locis are denoted by triangles.

2.7. Sanger sequencing

SARS-CoV-2 RNA was amplified using universal primers, and the products were subjected to agarose gel electrophoresis (2.5% agarose gel). DNA fragments were recovered from the agarose gel using a DNA Recovery Kit (Tiangen, Beijing, China), and DNA sequencing was performed by Sangon (Shanghai, China).

3. Results

3.1. SNVs selection and establishment of ARMS-PCR

To develop the diagnostic assay, we selected 10 key RBD SNVs (Fig. 1) that involved all the VOCs (Table S2) reported by the WHO. Several studies have reported that these SNVs enhance the virus' binding affinity to the host angiotensin-converting enzyme 2 receptor, as well as increase transmissibility and immune evasion (Faria et al., 2021; Harvey et al., 2021; Liu et al., 2021; McCallum et al., 2021; Motozono et al., 2021; Thomson et al., 2021; Wang et al., 2021; Yang et al., 2021; Yuan et al., 2021; Zhou et al., 2021; Zhu et al., 2021).

We designed 20 ARMS-PCR forward primers based on the selected SNVs. Two sets of primers were designed for each SNV locus, consisting of a wild-type forward primer and a mutant forward primer, as well as a universal reverse primer. ARMS-PCR systems were developed for the 10 SNVs loci, and the detection capacity of the wild-type and mutant primers were considerably different depending on whether wild-type (Fig. S1a) or mutant SARS-CoV-2 (Fig. S1b) was used as template. Moreover, we found that even if an amplification block was present to identify primer-template mismatches, it could not entirely prevent amplification but instead produced an increase in quantification cycle (Cq) values. These findings indicated that the amplification of wild-type and mutant primers should be considered when identifying SNV loci during microsphere phase amplification (MPA). Consequently, the wild-type and mutant forward primer for each SNV locus were coated on distinct microspheres (Fig. 1).

The amino-modified oligonucleotides selected for this study were coated to commercial fluorescent carboxylate microspheres via strong and high temperature-resistant covalent amide bonds (Dua et al., 2011; Ismail et al., 2021; Tan et al., 2021). We exploited the powerful multiple capabilities of the fluorescence-coded microspheres (Dobano et al., 2021) to detect multiple SNVs of SARS-CoV-2 VOCs.

3.2. Designing the multiplex MPA platform

The principle of multiplex MPA (MMPA) is schematically illustrated in Fig. 2. First, the RNA of wild-type SARS-CoV-2 or its variants was acquired, and asymmetric reverse transcription PCR (RT-PCR) was performed using a universal primer set targeting the RBD gene to enrich single-stranded DNA as a template for MMPA (Fig. 2a). MMPA was carried out in a single tube containing 20 types of primer-encoding microspheres, one wild-type primer coated and one mutant primer coated microspheres correspond to each SNV, and these microspheres

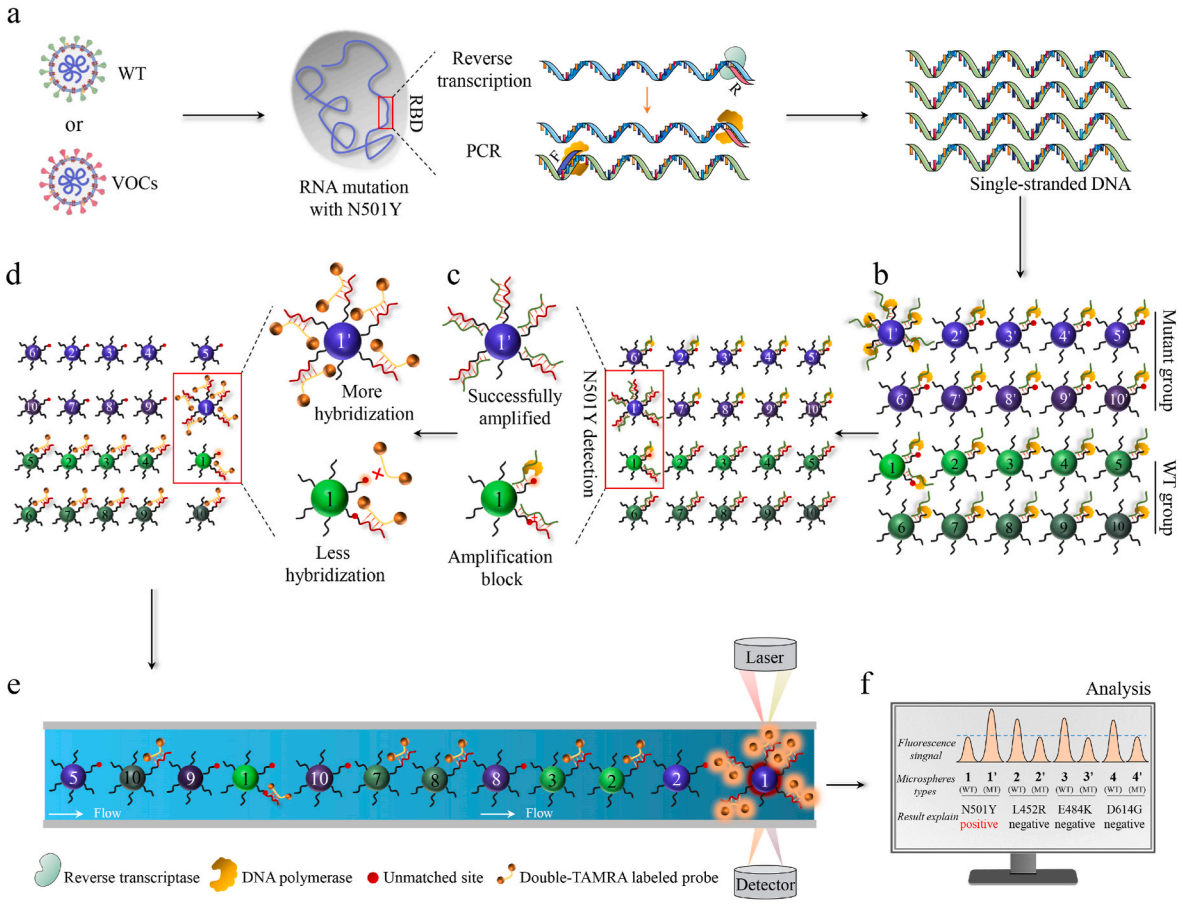

Fig. 2. Schematic representation of using MMPA to detect SARS-CoV-2 mutations. Taking the N501Y mutation as an example, the RNA of a SARS-CoV-2 variant strain with an N501Y mutation was isolated and transcribed into cDNA using reverse transcriptase. Following asymmetric PCR amplification, a large amount of single-stranded DNA was generated (a) and used in the MMPA assay with 20 primer-coated distinct microspheres in one reaction tube (b). Following MMPA, mutant-coated microspheres produced more amplification products than wild-type (WT)-coated microspheres (c). The amplified products were hybridized with dual-labeled fluorescent reporter probes (d) and detected using a Luminex 200 (e). The fluorescence levels on the surface of wild-type- and mutant-coated microspheres were compared to determine the N501Y mutation (f).

were divided into wild-type and mutant groups according to the primer type used (Fig. 2b). We noted that VOC RNA as the test template generated a higher number of amplification products than the wild-type RNA on the surface of their corresponding microspheres (Fig. 2c). Next, the amplified products were hybridized with the dual-labeled fluorescent reporter probe (Fig. 2d). The 20 types of differently coated microspheres were then mixed with sheath solution and passed through the micron pipeline one at a time (Fig. 2e). Primer coded microspheres were decoded by the red laser based sensor and the report hybridization probe was detected by green laser based sensor (Fig. 2e). Analysis was performed by comparing the fluorescence intensity on the surfaces of wild-type- and mutant-coated microspheres to differentiate among the SARS-CoV-2 variants (Fig. 2f).

3.3. Development and optimization of the MMPA platform

Several key factors, including primer density, carbon spacer length, annealing temperature, and reaction volume (Adessi et al., 2000; Chin et al., 2017; Drobyshev et al., 2009), were optimized to improve the amplification efficiency of MPA. An intensity that was too high (Fig. S2a) or too low (Fig. S2b) was unfavorable and inhibited the template from binding to the primer during MPA. We first determined the optimal primer density. The median reporter fluorescence intensity (MFI) at various primer labeling concentrations was monitored using the method shown in Fig. S2c. The results revealed that MFI was highest at a primer labeling concentration of 0.5 pmol (Fig. S2d). Secondly, carbon spacer lengths ranging from C0 to C36 at the 5′ end of the forward primer (Fig. S2e) were evaluated, as steric hindrance between immobilized primers and DNA polymerase is one of the major factors affecting MPA efficiency. As shown in Fig. S2e, the proportion of positive microspheres (PPM) increased. The highest PPM was obtained with a carbon spacer length of C36, suggesting a decrease in steric hindrance and gradual improvement in MPA efficiency. Thirdly, we examined the effect of annealing temperatures ranging from 47.3 °C to 69.5 °C. As shown in Fig. S2f, the highest ΔMFI (positive MFI minus negative MFI) was obtained at 55 °C. Finally, the reaction volume was evaluated, as this parameter can affect the probability of contact between DNA polymerase and the template-primer complex, which would influence the amplification efficiency of MPA. The data obtained showed that ΔMFI increased in reaction volumes up to 25 μL (Fig. S2g), confirming that a smaller reaction volume enhanced amplification efficiency.

Next, we established a singleplex MPA system based on the optimized parameters above and ARMS-PCR. Singleplex MPA was performed independently for each of the 10 SNV loci. The MFI corresponding to the wild-type primer-coated microsphere was higher than that of the mutant primer-coated microsphere when using wild-type SARS-CoV-2 as template but lower when using mutant SARS-CoV-2 as template (Fig. S3). As a result, these primers were able to identify a single site that allowed the mutant SARS-CoV-2 to be precisely differentiated from the wild-type SARS-CoV-2. These primers were consequently chosen for MMPA assembly.

MMPA was performed using 20 primer-coated microspheres in a single reaction tube under optimized reaction conditions. We discovered that including an addtional 0.4 μM of reverse primers in the reaction system considerably improved the fluorescence signal of positive amplification during MMPA (Fig. S4a). Furthermore, the highest MFI was obtained using 5 μL of pre-enriched template; this value subsequently decreased in higher input volumes (Fig. S4b). Enzyme concentrations of 1 U SS Taq and 10 U HS Taq DNA polymerase were determined to be optimal during MMPA (Fig. S4c). We also examined the effect of using several reporter probes instead of one universal dual-labeled fluorescent reporter probe on the signal intensity. The results indicated that using several reporter probes that target different RBD segments considerably improved the positive fluorescence signal (Fig. S4d), consistent with previously published literature (Fozouni et al., 2021). The optimized reaction conditions above ensured the excellent amplification efficiency and robustness of the MMPA platform, and were employed in subsequent experiments.

3.4. MMPA assay is highly sensitive in detecting SARS-CoV-2 RNA

The threshold of the MMPA assay for SARS-CoV-2 detection was evaluated using a 10-fold serial dilution of RNA samples from the natural wild-type and artificially constructed 10 SNV loci mutation SARS-CoV-2. The N1, N2, and N3 reverse transcription polymerase chain reaction (RT-PCR) primers and probes reported by the CDC (USA) were used as references (Lu et al., 2020). Our results revealed a lower limit of detection (LLOD) of 28 copies/reaction for wild-type SARS-CoV-2 RNA using both the CDC RT-PCR (Fig. 3a, b, c) and MMPA (Fig. 3d) assays. Similarly, the LLOD of the MMPA assay reached 28 copies/reaction for mutant SARS-CoV-2 RNA (Fig. 3e). The LLOD of sequencing was also consistent with MMPA (Table S3). These findings suggest that the sensitivity of the MMPA assay is equivalent to that of conventional RT-PCR and sequencing.

3.5. MMPA assay can successfully discriminate between wild-type and mutant SARS-CoV-2

We verified the ability of the MMPA assay to discriminate among the 10 SNVs of SARS-CoV-2. The results indicated that the standardized values of the 10 SNV loci were all negative when using natural wild-type SARS-CoV-2 RNA (Fig. 4a), suggesting a poor amplification efficiency of mutant primers in identifying wild-type SARS-CoV-2 RNA. However, when all 10 SNV loci of SARS-CoV-2 mutants, the amplification efficiency of wild-type primers was poor, and the standardized values of these SNVs were positive (Fig. 4b). Furthermore, we evaluated the ability of the MMPA assay to identify a single-site mutation in the 10 SNVs. The results revealed that the mutant SNV loci produced positive standardized values, whereas the wild-type SNV loci presented negative standardized values (Fig. 4c–l). The sequencing data were also consistent with the results of the MMPA assay (Fig. S5).

3.6. Detecting SARS-CoV-2 VOC pseudoviruses in simulated clinical samples

Performance testing of the MMPA assay in simulated clinical samples was carried out to verify its detection efficiency. We created pseudoviruses carrying the SARS-CoV-2 variant RNA sequence using techniques described in earlier papers (Wang et al., 2016). RNA samples extracted from SARS-CoV-2 VOC pseudoviruses or a control pseudovirus that were all spiked initially with nasal swabs eluent from healthy adults (Fig. 5a) were tested. The MMPA assay correctly identified the six VOCs, and the data were consistent with the sequencing results (Fig. 5b–g, S6). Both the negative and positive coincidence rates were at 100% (Table S4), highlighting the accurate discriminating qualities of the MMPA assay and its potential applications in the testing of actual clinical samples.

3.7. MMPA assay has good mutation discrimination and specificity for natural virus RNA detection

To assess the ability of MMPA assay to detect natural virus, RNA from the Delta variant (B.1.617.2), wild-type SARS-CoV-2 and a panel of other respiratory pathogens were analyzed via MMPA. The outcome was the inversion of the fluorescence signal in L452R, T478K and D614G sites of the Delta variant when compared with wild-type SARS-CoV-2 (Fig. 6a). This suggests a possible single-base mutation in these sites. The accuracy of the MMPA results was further validated via sequencing (Fig. 6b). All of the virus strains from a respiratory pathogen panel tested negative via MMPA (Fig. 6a). This analysis suggests that the MMPA assay provides excellent specificity.

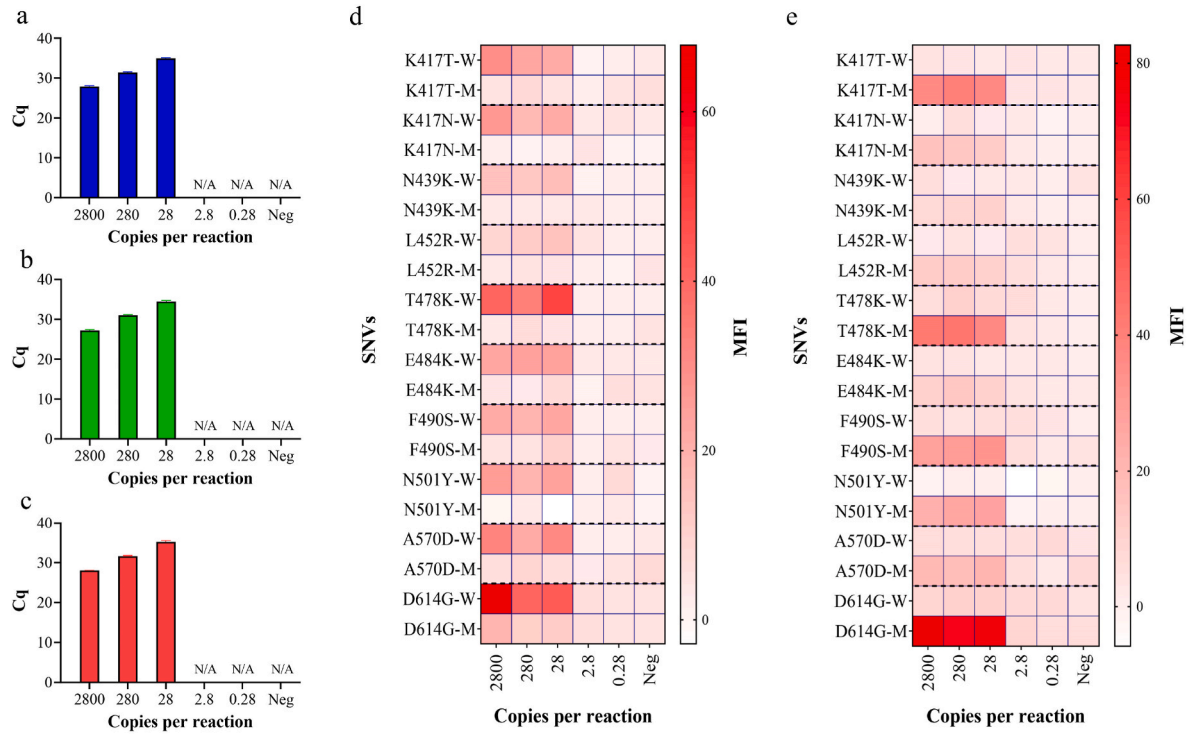

Fig. 3. Sensitivity analysis of the SARS-CoV-2 RNA detection system. The quantification cycle (Cq) values derived from the N1 (a), N2 (b), and N3 (c) reverse transcription polymerase chain reaction (RT-PCR) detection systems are shown. MMPA was performed to detect wild-type (d) or mutant (e) SARS-CoV-2 RNA, and the MFI from 20 primer-coated microspheres was measured using a Luminex 200. The experiments were repeated three times. Error bars represent the means ± standard deviations. N/A: not detected, Neg: negative control.

4. Discussion

The COVID-19 epidemic, caused by SARS-CoV-2, has continued to spread worldwide since the existence of the virus was reported in December 2019. However, as an RNA virus, SARS-CoV-2 is prone to errors in its genetic code during replication (Duffy, 2018), accumulating one to two nucleotide mutations every month (Li et al., 2020). When mutations occur in important segments such as the RBD, they may increase the virulence or transmissibility of the virus and become VOCs, resulting in the sudden aggravation of the situation (Becerra-Flores and Cardozo, 2020; Duchene et al., 2020; Tian et al., 2021). Therefore, it is crucial to monitor VOCs for several reasons, including promoting epidemic warning and epidemiological research, adjusting vaccine strategies, and optimizing diagnostic reagents.

In the present study, we established a method that can simultaneously detect SARS-CoV-2 RNA and distinguish important SNVs in the RBD of VOCs. Several innovative features of our design address the problem of mutual interference in multiplex PCR that seriously affects its sensitivity and specificity. We propose a new SNV detection strategy to deal with the inability of traditional ARMS-PCR to achieve 100% block in mutation detection.

Firstly, faced with the need for a multiplex detection system, we first established MMPA technology on the surface of microspheres. Primers for a specific SNV were coated on corresponding microspheres, i.e., only this SNV would be distinguished by these microspheres. This one-to-one (i.e., SNV-to-microspheres) matched amplification approach established a foundation for achieving multiple parallel amplification reactions. Because of a low probability of collision between microspheres, the probability of nonspecific amplification among numerous primers limited in microspheres would be significantly reduced. Therefore, even if dozens of distinct microspheres were co-amplified in a single reaction, they would not interfere with one another.

Secondly, as the ARMS-PCR method used to detect mutations failed to achieve a 100% block, we adopted the double primer-coded microsphere strategy to improve detection accuracy. That is, two microspheres were used as a group, targeted at the mutant and wild-type SARS-CoV-2 detection sites. Regardless of the blocking efficiency, more robust amplification must occur on the surface of microspheres without amplification blocking. Therefore, the presence of mutations can be determined by comparing the amplification intensity of microspheres corresponding to the wild-type and mutant templates. As the microspheres used in the study contained up to 500, the number of microspheres used can meet the detection needs of most multiple SNVs even when adopting a dual strategy.

This innovative approach gives MMPA several critical advantages over other sensing technologies and gold standard sequencing with regard to SARS-CoV-2 SNV detection. More SNV loci can be detected in parallel, better sensitivity and specificity are provided, a simpler and more streamlined workflow is used, the technology is more suitable for clinical applications, and the SNV locus detection panel can be updated quickly to account for newly emerged strains.

Currently reported SARS-CoV-2 detection sensors include immune- and nucleic acid based sensors. The advantage of immunoassay sensor is that the suitable for POCT application. However, it cannot be used to distinguish mutant strains at present. A few sensors based on nucleic acid testing can be used for SNV detection, but they can only distinguish a single mutation site and cannot meet the needs of the current situation in which multiple mutants are prevalent. In addition, most of these sensors perform single-channel detection and are not suitable for large scale analysis (Table S5). The method described herein offers the advantage that the theoretical maximum number of SNVs analyzed using one MMPA test can reach 250, and each round can include up to 95 tests.

The method developed here differs from the xMAP mutation detection method. The latter only removes the limit of “number of detection channels” during the product detection process through hybridization between the different microspheres and amplification products (Hu et al., 2012). xMAP does not provide an effective way to avoid

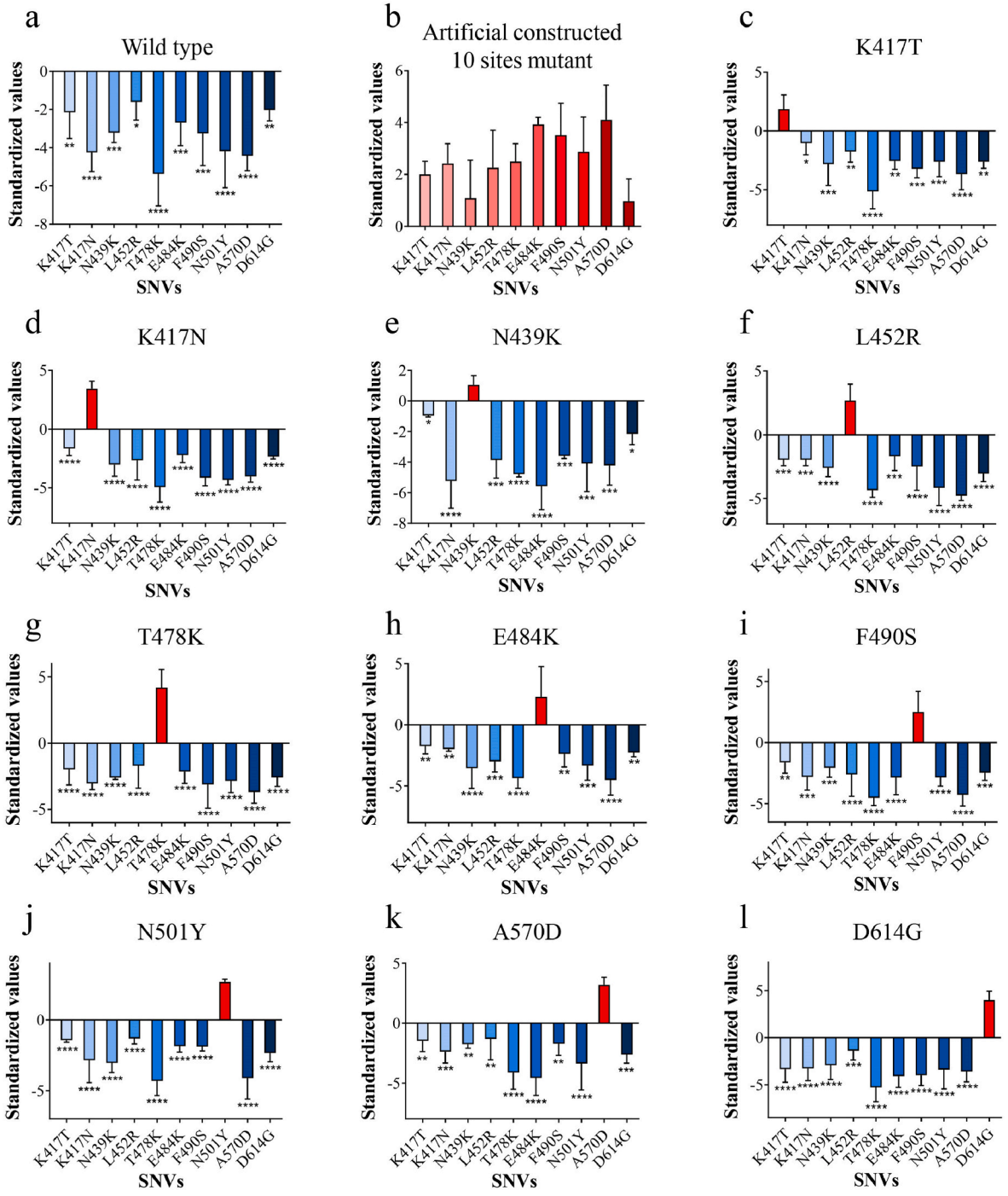

Fig. 4. Evaluation of the discriminative performance of the MMPA assay. The wild-type SARS-CoV-2 (a) or 10 SNV loci of mutated SARS-CoV-2 RNA (b) were detected using the MMPA assay. In addition, mutations of SARS-CoV-2 at a single site were identified through the MMPA assay (c–l). Data are expressed as mean ± standard deviation (n = 3). Statistical analysis was performed by one-way analysis of variance (ANOVA) using GraphPad Prism 8 software (*P < 0.05, **P < 0.01, ***P < 0.001, ****P < 0.0001).

interference among sequences on a multiple detection platform, which is critical to the sensitivity of the system. Once generated, nonspecific amplification would compete with specific amplification, consequently decreasing detection sensitivity (Fig. S7). Most previous studies on the xMAP mutation detection system mainly focused on genetic disease diagnoses (Schwartz et al., 2009), and SNV-related drug resistance testing (Carnevale et al., 2007). This type of mutation detection system is characterized by a high load of the template to be tested and a relatively low demand for the sensitivity of the detection system. The application of this method in pathogen detection will result in missed detection of low load samples and inaccurate monitoring of mutation sites. The analytical sensitivity of MMPA was tested and essentially displayed the same sensitivity as the SARS-CoV-2 detection system proposed by the CDC (U.S.A), thereby meeting the requirements for accurate pathogen detection (Table S6).

Currently, sequencing is the gold standard for detecting SARS-CoV-2 SNVs. Here, we selected sequencing as a reference technique to evaluate the analytical performance of the MMPA system using spiked RNA samples. The results of MMPA were consistent with those obtained by sequencing, regardless of the varying RNA loads or SNV loci. However,

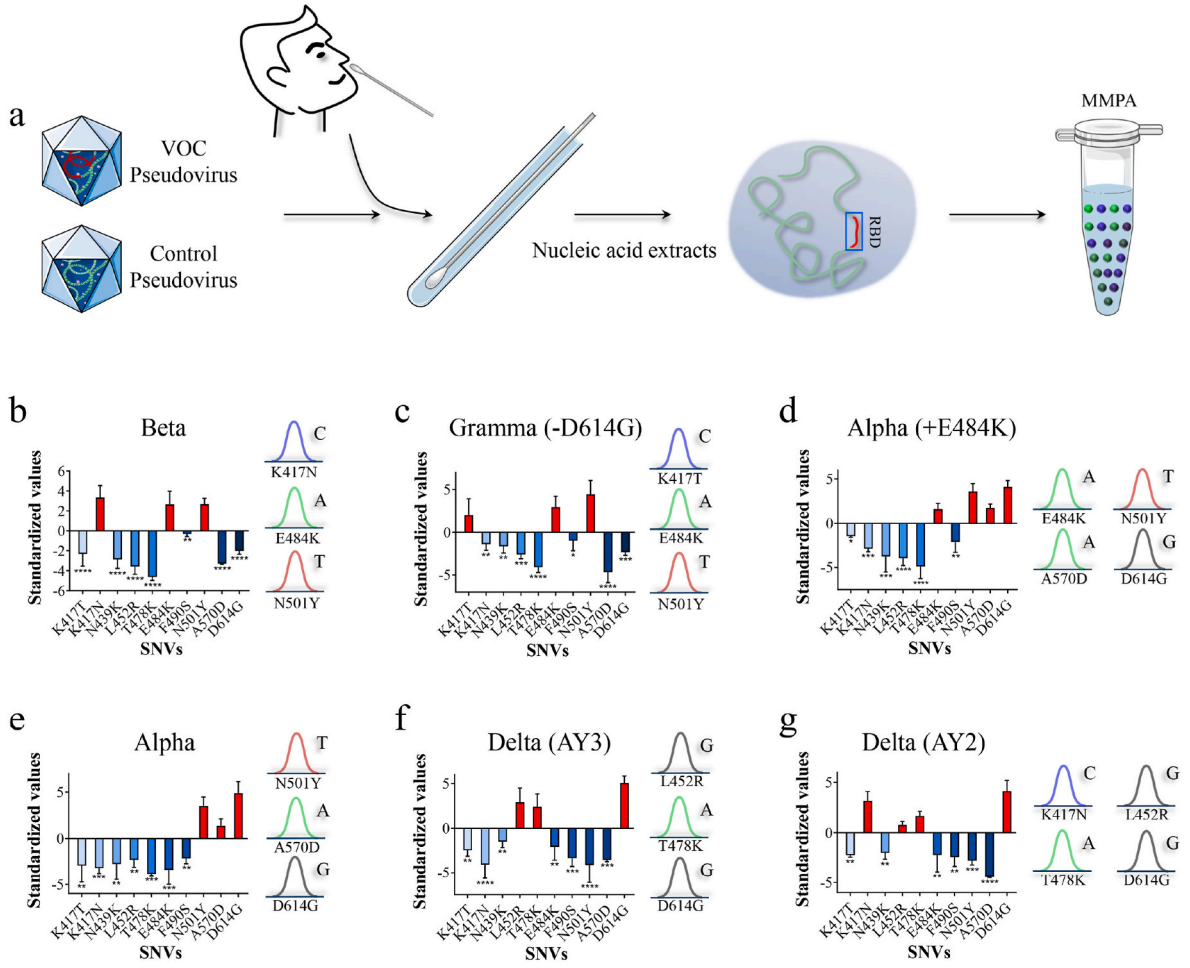

Fig. 5. Performance testing of the MMPA assay in simulated clinical samples. The SARS-CoV-2 VOC pseudovirus or control pseudovirus was spiked with nasal swabs eluent from healthy humans, and nucleic acids were extracted and analyzed by MMPA (a). The MMPA results were compared to sequencing data for different VOCs (b–g). The experiments were repeated three times. The error bars represent means ± standard deviations. Statistical analysis was performed by one-way analysis of variance (ANOVA) using GraphPad Prism 8 software (*P < 0.05, **P < 0.01, ***P < 0.001, ****P < 0.0001).

sequencing equipment is not commonly available in clinical settings. Only qualified clinical testing units attached to scientific research facilities would likely be equipped with a sequencer. Therefore, the clinical application of sequencing-dependent SNV detection methods is limited. Conversely, the detection equipment of microsphere used in this study has been routinely employed in many clinical units, as well as widely used in cytokine detection (Montoya et al., 2017), HPV typing (Pesic et al., 2020; Zhao et al., 2017), and SARS-CoV-2 serosurveillance (Marien et al., 2021). Therefore, it is easier to promote the MMPA system in clinical applications. Moreover, detection processes involving Sanger sequencing, high-throughput sequencing, and single-molecule sequencing are complex, costly, and time-consuming. The data generated through these methods are also difficult to analyze. By contrast, MMPA can generate results in only 4 h from acquiring the RNA template, and the operation and data interpretation are relatively simple. Although the MMPA system cannot be used to discover nascent SNV, it can complement sequencing technologies. For example, once a new SNV is identified by sequencing, the MMPA platform could update its detection panel immediately, without compromising compatibility between primers. Vice versa, MMPA platform can be used to detect a wide range of SNVs in multiple runs and preliminarily classify samples according to known variants. Only a small number of samples selected from each class will require further sequencing to obtain the sequence information of the predominant strain. Therefore, the representation and pertinence of the samples selected for sequencing will be improved, and the total number of generated sequences will be considerably reduced.

Except for sequencing, one limitation of most multiple nucleic acid detection methods is maintaining high sensitivity in a multiplex amplification system. This limitation can be overcome by ensuring that the numerous primers for different targets do not interfere with one another. The quintessence of MMPA technology is to use microparticles as carriers to provide relatively independent amplification space for each target and to achieve multi-parallel amplification and detection using a 500 × array. Therefore, the MMPA technology has the potential for further expansion. Future work will include developing the applications of MMPA in multi-locus SNP detection, syndrome pathogen identification detection, and genotyping.

5. Conclusion

In the present study, we developed an encodable MMPA sensing platform to detect SARS-CoV-2 and simultaneously identify 10 key SNVs in the RBD by combining primer-coded microsphere technology with a dual fluorescence decoding strategy. This assay harnessed the principle of the separation of physical space to selectively amplify different SNVs on distinct microspheres, avoiding the mutual interference between pairs of primers to achieve multiple amplification within a single reaction. Compared to traditional real-time fluorescent qPCR, the sensitivity of the assay reached a low detection level of 28 copies/reaction, and its

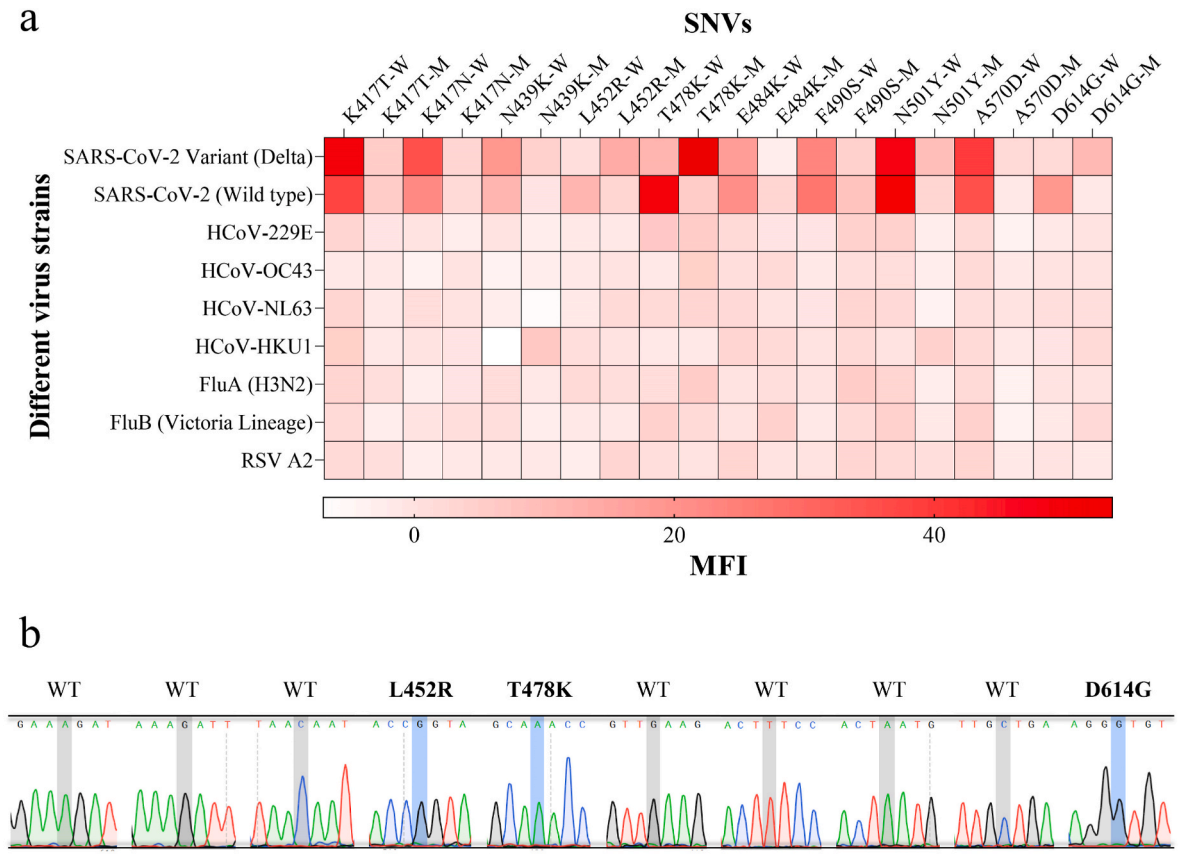

Fig. 6. Using the MMPA assay to identify the Delta variant in natural virus RNA. Results of testing MMPA with different virus strains (a). The Delta variant Sequencing result (b). Experiments were repeated three times with similar results.

detection capability was expanded to offer multiple parallel SNV detection with a relatively high accuracy level. The positive and negative concordance rates were all 100% compared to the gold standard of sequencing. From a theoretical perspective, MMPA can be designed to detect more SNVs, as long as the mutation sites are known. In other words, the rapid performance of MMPA can be exploited when responding to an outbreak of SARS-CoV-2 variants. In summary, MMPA has a short turn-around time, offers high efficiency, sensitivity, accuracy, and throughput, and has the potential to detect different types of pathogens. Thus, the simple design of MMPA can be quickly modified to target any emerging infectious diseases.

CRediT authorship contribution statement

Zecheng Zhong: Established and optimized the MMPA sensing platform. Integrated the data and wrote the manuscript. **Jin Wang:** Established and optimized the MMPA sensing platform. Integrated the data and wrote the manuscript. **Shuizhen He:** Established and optimized the MMPA sensing platform. Integrated the data and wrote the manuscript. **Xiaosong Su:** Helped to perform SARS-CoV-2 mutation detection. **Weida Huang:** Helped to perform SARS-CoV-2 mutation detection. **Zhihao Zhuo:** Helped to perform SARS-CoV-2 mutation detection. **Xiaomei Zhu:** Helped to perform SARS-CoV-2 mutation detection. **Mujin Fang:** Helped to perform SARS-CoV-2 mutation detection. **Tingdong Li:** Helped to prepare the figures. **Shiyin Zhang:** Conceptualized the project and designed the experiments. Provided critical revision of the manuscript for important intellectual content. **Shengxiang Ge:** Conceptualized the project and designed the experiments. Approved the final version of the manuscript. **Jun Zhang:** Approved the final version of the manuscript. **Ningshao Xia:** Conceptualized the project and designed the experiments. Approved the final version of the manuscript.

Declaration of competing interest

The authors declare that they have no known competing financial interests or personal relationships that could have appeared to influence the work reported in this paper.

Acknowledgements

This study was supported by National Natural Science Foundation of China (62003284), President Fund of Xiamen University (20720210089) and the CAMS Innovation Fund for Medical Sciences (2019RU022).

Appendix A. Supplementary data

Supplementary data to this article can be found online at https://doi.org/10.1016/j.bios.2022.114032.

References

Adessi, C., Matton, G., Ayala, G., Turcatti, G., Mermod, J.J., Mayer, P., Kawashima, E., 2000. Solid phase DNA amplification: characterisation of primer attachment and amplification mechanisms. Nucleic Acids Res. 28 (20), E87.
Afzal, A., 2020. Molecular diagnostic technologies for COVID-19: limitations and challenges. J. Adv. Res. 26, 149–159.
Ahmadivand, A., Gerislioglu, B., Ramezani, Z., Kaushik, A., Manickam, P., Ghoreishi, S. A., 2021. Functionalized terahertz plasmonic metasensors: femtomolar-level detection of SARS-CoV-2 spike proteins. Biosens. Bioelectron. 177, 112971.
Ai, T., Yang, Z., Hou, H., Zhan, C., Chen, C., Lv, W., Tao, Q., Sun, Z., Xia, L., 2020. Correlation of chest ct and RT-PCR testing for coronavirus disease 2019 (COVID-19) in China: a report of 1014 cases. Radiology 296 (2), E32–E40.

Becerra-Flores, M., Cardozo, T., 2020. SARS-CoV-2 viral spike G614 mutation exhibits higher case fatality rate. Int. J. Clin. Pract. 74 (8), e13525.
Board, R.E., Thelwell, N.J., Ravetto, P.F., Little, S., Ranson, M., Dive, C., Hughes, A., Whitcombe, D., 2008. Multiplexed assays for detection of mutations in PIK3CA. Clin. Chem. 54 (4), 757–760.
Carnevale, E.P., Kouri, D., DaRe, J.T., McNamara, D.T., Mueller, I., Zimmerman, P.A., 2007. A multiplex ligase detection reaction-fluorescent microsphere assay for simultaneous detection of single nucleotide polymorphisms associated with Plasmodium falciparum drug resistance. J. Clin. Microbiol. 45 (3), 752–761.
Chin, W.H., Sun, Y., Hogberg, J., Hung, T.Q., Wolff, A., Bang, D.D., 2017. Solid-phase PCR for rapid multiplex detection of Salmonella spp. at the subspecies level, with amplification efficiency comparable to conventional PCR. Anal. Bioanal. Chem. 409 (10), 2715–2726.
Chuenkova, M.V., PereiraPerrin, M., 2009. Trypanosoma cruzi targets Akt in host cells as an intracellular antiapoptotic strategy. Sci. Signal. 2 (97), ra74.
Corman, V.M., Landt, O., Kaiser, M., Molenkamp, R., Meijer, A., Chu, D.K., Bleicker, T., Brunink, S., Schneider, J., Schmidt, M.L., Mulders, D.G., Haagmans, B.L., van der Veer, B., van den Brink, S., Wijsman, L., Goderski, G., Romette, J.L., Ellis, J., Zambon, M., Peiris, M., Goossens, H., Reusken, C., Koopmans, M.P., Drosten, C., 2020. Detection of 2019 novel coronavirus (2019-nCoV) by real-time RT-PCR. Euro Surveill. 25 (3).
Dobano, C., Vidal, M., Santano, R., Jimenez, A., Chi, J., Barrios, D., Ruiz-Olalla, G., Rodrigo Melero, N., Carolis, C., Parras, D., Serra, P., Martinez de Aguirre, P., Carmona-Torre, F., Reina, G., Santamaria, P., Mayor, A., Garcia-Basteiro, A.L., Izquierdo, L., Aguilar, R., Moncunill, G., 2021. Highly sensitive and specific multiplex antibody assays to quantify immunoglobulins M, A, and G against SARS-CoV-2 antigens. J. Clin. Microbiol. 59 (2).
Dorn, A.V., Cooney, R.E., Sabin, M.L., 2020. COVID-19 exacerbating inequalities in the US. Lancet 395 (10232), 1243–1244.
Drobyshev, A.L., Nasedkina, T.V., Zakharova, N.V., 2009. The role of DNA diffusion in solid phase polymerase chain reaction with gel-immobilized primers in planar and capillary microarray format. Biomicrofluidics 3 (4), 44112.
Dua, P., Kim, S., Lee, D.K., 2011. Nucleic acid aptamers targeting cell-surface proteins. Methods 54 (2), 215–225.
Duchene, S., Featherstone, L., Haritopoulou-Sinanidou, M., Rambaut, A., Lemey, P., Baele, G., 2020. Temporal signal and the phylodynamic threshold of SARS-CoV-2. Virus Evol. 6 (2), veaa061.
Duffy, S., 2018. Why are RNA virus mutation rates so damn high? PLoS Biol. 16 (8), e3000003.
Elnifro, E.M., Ashshi, A.M., Cooper, R.J., Klapper, P.E., 2000. Multiplex PCR: optimization and application in diagnostic virology. Clin. Microbiol. Rev. 13 (4), 559–570.
Esbin, M.N., Whitney, O.N., Chong, S., Maurer, A., Darzacq, X., Tjian, R., 2020. Overcoming the bottleneck to widespread testing: a rapid review of nucleic acid testing approaches for COVID-19 detection. RNA 26 (7), 771–783.
Faria, N.R., Mellan, T.A., Whittaker, C., Claro, I.M., Candido, D.D.S., Mishra, S., Crispim, M.A.E., Sales, F.C.S., Hawryluk, I., McCrone, J.T., Hulswit, R.J.G., Franco, L.A.M., Ramundo, M.S., de Jesus, J.G., Andrade, P.S., Coletti, T.M., Ferreira, G.M., Silva, C.A.M., Manuli, E.R., Pereira, R.H.M., Peixoto, P.S., Kraemer, M.U.G., Gaburo Jr., N., Camilo, C.D.C., Hoeltgebaum, H., Souza, W.M., Rocha, E.C., de Souza, L.M., de Pinho, M.C., Araujo, L.J.T., Malta, F.S.V., de Lima, A. B., Silva, J.D.P., Zauli, D.A.G., Ferreira, A.C.S., Schnekenberg, R.P., Laydon, D.J., Walker, P.G.T., Schluter, H.M., Dos Santos, A.L.P., Vidal, M.S., Del Caro, V.S., Filho, R.M.F., Dos Santos, H.M., Aguiar, R.S., Proenca-Modena, J.L., Nelson, B., Hay, J.A., Monod, M., Miscouridou, X., Coupland, H., Sonabend, R., Vollmer, M., Gandy, A., Prete Jr., C.A., Nascimento, V.H., Suchard, M.A., Bowden, T.A., Pond, S.L. K., Wu, C.H., Ratmann, O., Ferguson, N.M., Dye, C., Loman, N.J., Lemey, P., Rambaut, A., Fraiji, N.A., Carvalho, M., Pybus, O.G., Flaxman, S., Bhatt, S., Sabino, E.C., 2021. Genomics and epidemiology of the P.1 SARS-CoV-2 lineage in Manaus, Brazil. Science 372 (6544), 815–821.
Fozouni, P., Son, S., Diaz de Leon Derby, M., Knott, G.J., Gray, C.N., D'Ambrosio, M.V., Zhao, C., Switz, N.A., Kumar, G.R., Stephens, S.I., Boehm, D., Tsou, C.L., Shu, J., Bhuiya, A., Armstrong, M., Harris, A.R., Chen, P.Y., Osterloh, J.M., Meyer-Franke, A., Joehnk, B., Walcott, K., Sil, A., Langelier, C., Pollard, K.S., Crawford, E. D., Puschnik, A.S., Phelps, M., Kistler, A., DeRisi, J.L., Doudna, J.A., Fletcher, D.A., Ott, M., 2021. Amplification-free detection of SARS-CoV-2 with CRISPR-Cas13a and mobile phone microscopy. Cell 184 (2), 323–333 e329.
Grubaugh, N.D., Hodcroft, E.B., Fauver, J.R., Phelan, A.L., Cevik, M., 2021. Public health actions to control new SARS-CoV-2 variants. Cell 184 (5), 1127–1132.
Harvey, W.T., Carabelli, A.M., Jackson, B., Gupta, R.K., Thomson, E.C., Harrison, E.M., Ludden, C., Reeve, R., Rambaut, A., Consortium, C.-G.U., Peacock, S.J., Robertson, D.L., 2021. SARS-CoV-2 variants, spike mutations and immune escape. Nat. Rev. Microbiol. 19 (7), 409–424.
Hu, X., Zhang, Y., Zhou, X., Xu, B., Yang, M., Wang, M., Zhang, C., Li, J., Bai, R., Xu, W., Ma, X., 2012. Simultaneously typing nine serotypes of enteroviruses associated with hand, foot, and mouth disease by a GeXP analyzer-based multiplex reverse transcription-PCR assay. J. Clin. Microbiol. 50 (2), 288–293.
Ismail, A.R., Kashtoh, H., Baek, K.H., 2021. Temperature-resistant and solvent-tolerant lipases as industrial biocatalysts: biotechnological approaches and applications. Int. J. Biol. Macromol. 187, 127–142.
Jayamohan, H., Lambert, C.J., Sant, H.J., Jafek, A., Patel, D., Feng, H., Beeman, M., Mahmood, T., Nze, U., Gale, B.K., 2021. SARS-CoV-2 pandemic: a review of molecular diagnostic tools including sample collection and commercial response with associated advantages and limitations. Anal. Bioanal. Chem. 413 (1), 49–71.
Ju, J.H., Oh, S., Lee, K.M., Yang, W., Nam, K.S., Moon, H.G., Noh, D.Y., Kim, C.G., Park, G., Park, J.B., Lee, T., Arteaga, C.L., Shin, I., 2015. Cytokeratin19 induced by HER2/ERK binds and stabilizes HER2 on cell membranes. Cell Death Differ. 22 (4), 665–676.
Kaushik, A., 2021. Manipulative magnetic nanomedicine: the future of COVID-19 pandemic/endemic therapy. Expet Opin. Drug Deliv. 18 (5), 531–534.
Khodakov, D., Li, J., Zhang, J.X., Zhang, D.Y., 2021. Highly multiplexed rapid DNA detection with single-nucleotide specificity via convective PCR in a portable device. Nat. Biomed. Eng. 5 (7), 702–712.
Kumar, M., Gulati, S., Ansari, A.H., Phutela, R., Acharya, S., Azhar, M., Murthy, J., Kathpalia, P., Kanakan, A., Maurya, R., Vasudevan, J.S., S, A., Pandey, R., Maiti, S., Chakraborty, D., 2021. FnCas9-based CRISPR diagnostic for rapid and accurate detection of major SARS-CoV-2 variants on a paper strip. Elife 10.
Li, Q., Wu, J., Nie, J., Zhang, L., Hao, H., Liu, S., Zhao, C., Zhang, Q., Liu, H., Nie, L., Qin, H., Wang, M., Lu, Q., Li, X., Sun, Q., Liu, J., Zhang, L., Li, X., Huang, W., Wang, Y., 2020. The impact of mutations in SARS-CoV-2 spike on viral infectivity and antigenicity. Cell 182 (5), 1284–1294 e1289.
Little, S., 2001. Amplification-refractory mutation system (ARMS) analysis of point mutations. Curr. Protoc. Hum. Genet. Chapter 9. Unit 9 8.
Liu, Y., Liu, J., Plante, K.S., Plante, J.A., Xie, X., Zhang, X., Ku, Z., An, Z., Scharton, D., Schindewolf, C., Menachery, V.D., Shi, P.Y., Weaver, S.C., 2021. The N501Y Spike Substitution Enhances SARS-CoV-2 Transmission. bioRxiv.
Lu, X., Wang, L., Sakthivel, S.K., Whitaker, B., Murray, J., Kamili, S., Lynch, B., Malapati, L., Burke, S.A., Harcourt, J., Tamin, A., Thornburg, N.J., Villanueva, J.M., Lindstrom, S., 2020. US CDC real-time reverse transcription PCR panel for detection of severe acute respiratory syndrome coronavirus 2. Emerg. Infect. Dis. 26 (8).
Marien, J., Ceulemans, A., Michiels, J., Heyndrickx, L., Kerkhof, K., Foque, N., Widdowson, M.A., Mortgat, L., Duysburgh, E., Desombere, I., Jansens, H., Van Esbroeck, M., Arien, K.K., 2021. Evaluating SARS-CoV-2 spike and nucleocapsid proteins as targets for antibody detection in severe and mild COVID-19 cases using a Luminex bead-based assay. J. Virol Methods 288, 114025.
McCallum, M., Bassi, J., De Marco, A., Chen, A., Walls, A.C., Di Iulio, J., Tortorici, M.A., Navarro, M.J., Silacci-Fregni, C., Saliba, C., Sprouse, K.R., Agostini, M., Pinto, D., Culap, K., Bianchi, S., Jaconi, S., Cameroni, E., Bowen, J.E., Tilles, S.W., Pizzuto, M. S., Guastalla, S.B., Bona, G., Pellanda, A.F., Garzoni, C., Van Voorhis, W.C., Rosen, L. E., Snell, G., Telenti, A., Virgin, H.W., Piccoli, L., Corti, D., Veesler, D., 2021. SARS-CoV-2 immune evasion by the B.1.427/B.1.429 variant of concern. Science 373 (6555), 648–654.
Mishra, K.K., Patel, P., Bhukhanvala, D.S., Shah, A., Ghosh, K., 2017. A multiplex ARMS PCR approach to detection of common beta-globin gene mutations. Anal. Biochem. 537, 93–98.
Montoya, J.G., Holmes, T.H., Anderson, J.N., Maecker, H.T., Rosenberg-Hasson, Y., Valencia, I.J., Chu, L., Younger, J.W., Tato, C.M., Davis, M.M., 2017. Cytokine signature associated with disease severity in chronic fatigue syndrome patients. Proc. Natl. Acad. Sci. U. S. A. 114 (34), E7150–E7158.
Motozono, C., Toyoda, M., Zahradnik, J., Saito, A., Nasser, H., Tan, T.S., Ngare, I., Kimura, I., Uriu, K., Kosugi, Y., Yue, Y., Shimizu, R., Ito, J., Torii, S., Yonekawa, A., Shimono, N., Nagasaki, Y., Minami, R., Toya, T., Sekiya, N., Fukuhara, T., Matsuura, Y., Schreiber, G., , The Genotype to Phenotype Japan (G2P-Japan) Consortium, Ikeda, T., Nakagawa, S., Ueno, T., Sato, K., 2021. SARS-CoV-2 spike L452R variant evades cellular immunity and increases infectivity. Cell Host Microbe 29 (7), 1124–1136 e1111.
Mujawar, M.A., Gohel, H., Bhardwaj, S.K., Srinivasan, S., Hickman, N., Kaushik, A., 2020. Nano-enabled biosensing systems for intelligent healthcare: towards COVID-19 management. Mater. Today Chem. 17, 100306.
Osorio, N.S., Correia-Neves, M., 2021. Implication of SARS-CoV-2 evolution in the sensitivity of RT-qPCR diagnostic assays. Lancet Infect. Dis. 21 (2), 166–167.
Pesic, A., Krings, A., Hempel, M., Preyer, R., Kaufmann, A.M., 2020. Clinical performance of the HPV DNA Array genotyping assay in detection of CIN2+ lesions with BS GP5+/6+ MPG Luminex tested cervical samples. J. Med. Virol. 92 (1), 113–118.
Schwartz, K.M., Pike-Buchanan, L.L., Muralidharan, K., Redman, J.B., Wilson, J.A., Jarvis, M., Cura, M.G., Pratt, V.M., 2009. Identification of cystic fibrosis variants by polymerase chain reaction/oligonucleotide ligation assay. J. Mol. Diagn. 11 (3), 211–215.
Sharma, P.K., Kim, E.S., Mishra, S., Ganbold, E., Seong, R.S., Kaushik, A.K., Kim, N.Y., 2021. Ultrasensitive and reusable graphene oxide-modified double-interdigitated capacitive (DIDC) sensing chip for detecting SARS-CoV-2. ACS Sens. 6 (9), 3468–3476.
Tahamtan, A., Ardebili, A., 2020. Real-time RT-PCR in COVID-19 detection: issues affecting the results. Expert Rev. Mol. Diagn 20 (5), 453–454.
Tan, T.K., Rijal, P., Rahikainen, R., Keeble, A.H., Schimanski, L., Hussain, S., Harvey, R., Hayes, J.W.P., Edwards, J.C., McLean, R.K., Martini, V., Pedrera, M., Thakur, N., Conceicao, C., Dietrich, I., Shelton, H., Ludi, A., Wilsden, G., Browning, C., Zagrajek, A.K., Bialy, D., Bhat, S., Stevenson-Leggett, P., Hollinghurst, P., Tully, M., Moffat, K., Chiu, C., Waters, R., Gray, A., Azhar, M., Mioulet, V., Newman, J., Asfor, A.S., Burman, A., Crossley, S., Hammond, J.A., Tchilian, E., Charleston, B., Bailey, D., Tuthill, T.J., Graham, S.P., Duyvesteyn, H.M.E., Malinauskas, T., Huo, J., Tree, J.A., Buttigieg, K.R., Owens, R.J., Carroll, M.W., Daniels, R.S., McCauley, J.W., Stuart, D.I., Huang, K.A., Howarth, M., Townsend, A.R., 2021. A COVID-19 vaccine candidate using SpyCatcher multimerization of the SARS-CoV-2 spike protein receptor-binding domain induces potent neutralising antibody responses. Nat. Commun. 12 (1), 542.
Thomson, E.C., Rosen, L.E., Shepherd, J.G., Spreafico, R., da Silva Filipe, A., Wojcechowskyj, J.A., Davis, C., Piccoli, L., Pascall, D.J., Dillen, J., Lytras, S., Czudnochowski, N., Shah, R., Meury, M., Jesudason, N., De Marco, A., Li, K., Bassi, J., O'Toole, A., Pinto, D., Colquhoun, R.M., Culap, K., Jackson, B., Zatta, F., Rambaut, A., Jaconi, S., Sreenu, V.B., Nix, J., Zhang, I., Jarrett, R.F., Glass, W.G.,

Beltramello, M., Nomikou, K., Pizzuto, M., Tong, L., Cameroni, E., Croll, T.I., Johnson, N., Di Iulio, J., Wickenhagen, A., Ceschi, A., Harbison, A.M., Mair, D., Ferrari, P., Smollett, K., Sallusto, F., Carmichael, S., Garzoni, C., Nichols, J., Galli, M., Hughes, J., Riva, A., Ho, A., Schiuma, M., Semple, M.G., Openshaw, P.J.M., Fadda, E., Baillie, J.K., Chodera, J.D., Investigators, I.C., Consortium, C.-G.U., Rihn, S.J., Lycett, S.J., Virgin, H.W., Telenti, A., Corti, D., Robertson, D.L., Snell, G., 2021. Circulating SARS-CoV-2 spike N439K variants maintain fitness while evading antibody-mediated immunity. Cell 184 (5), 1171–1187 e1120.

Tian, F., Tong, B., Sun, L., Shi, S., Zheng, B., Wang, Z., Dong, X., Zheng, P., 2021. N501Y mutation of spike protein in SARS-CoV-2 strengthens its binding to receptor ACE2. Elife 10.

Vandenberg, O., Martiny, D., Rochas, O., van Belkum, A., Kozlakidis, Z., 2021. Considerations for diagnostic COVID-19 tests. Nat. Rev. Microbiol. 19 (3), 171–183.

Wang, R., Chen, J., Gao, K., Wei, G.W., 2021. Vaccine-escape and fast-growing mutations in the United Kingdom, the United States, Singapore, Spain, India, and other COVID-19-devastated countries. Genomics 113 (4), 2158–2170.

Wang, R., Hozumi, Y., Yin, C., Wei, G.W., 2020. Mutations on COVID-19 diagnostic targets. Genomics 112 (6), 5204–5213.

Wang, S., Liu, Y., Li, D., Zhou, T., Gao, S., Zha, E., Yue, X., 2016. Preparation and evaluation of MS2 bacteriophage-like particles packaging hepatitis E virus RNA. FEMS Microbiol. Lett. 363 (20).

World Health Organization, 2021. Tracking SARS-CoV-2 variants. URL: https://www.who.int/en/activities/tracking-SARS-CoV-2-variants/.

Yang, T.J., Yu, P.Y., Chang, Y.C., Liang, K.H., Tso, H.C., Ho, M.R., Chen, W.Y., Lin, H.T., Wu, H.C., Hsu, S.D., 2021. Effect of SARS-CoV-2 B.1.1.7 mutations on spike protein structure and function. Nat. Struct. Mol. Biol. 28 (9), 731–739.

Yuan, M., Huang, D., Lee, C.D., Wu, N.C., Jackson, A.M., Zhu, X., Liu, H., Peng, L., van Gils, M.J., Sanders, R.W., Burton, D.R., Reincke, S.M., Pruss, H., Kreye, J., Nemazee, D., Ward, A.B., Wilson, I.A., 2021. Structural and functional ramifications of antigenic drift in recent SARS-CoV-2 variants. Science 373 (6556), 818–823.

Zhang, S., Su, X., Wang, J., Chen, M., Li, C., Li, T., Ge, S., Xia, N., 2020. Nucleic acid testing for coronavirus disease 2019: demand, research progression, and perspective. Crit. Rev. Anal. Chem. 1–12.

Zhao, P.Y., Jiang, H.C., Li, Y., Wang, J.B., Zhang, T.T., Liu, C.H., Song, L.W., Cheng, J.J., 2017. Comparison of the cervista HPV HR test and luminex XMAP technology for the diagnosis of cervical intraepithelial neoplasia. Eur. J. Obstet. Gynecol. Reprod. Biol. 214, 150–155.

Zhou, B., Thao, T.T.N., Hoffmann, D., Taddeo, A., Ebert, N., Labroussaa, F., Pohlmann, A., King, J., Steiner, S., Kelly, J.N., Portmann, J., Halwe, N.J., Ulrich, L., Trueb, B.S., Fan, X., Hoffmann, B., Wang, L., Thomann, L., Lin, X., Stalder, H., Pozzi, B., de Brot, S., Jiang, N., Cui, D., Hossain, J., Wilson, M.M., Keller, M.W., Stark, T.J., Barnes, J.R., Dijkman, R., Jores, J., Benarafa, C., Wentworth, D.E., Thiel, V., Beer, M., 2021. SARS-CoV-2 spike D614G change enhances replication and transmission. Nature 592 (7852), 122–127.

Zhu, X., Mannar, D., Srivastava, S.S., Berezuk, A.M., Demers, J.P., Saville, J.W., Leopold, K., Li, W., Dimitrov, D.S., Tuttle, K.S., Zhou, S., Chittori, S., Subramaniam, S., 2021. Cryo-electron microscopy structures of the N501Y SARS-CoV-2 spike protein in complex with ACE2 and 2 potent neutralizing antibodies. PLoS Biol. 19 (4), e3001237.